JOURNAL OF VIROLOGY, Mar. 2010, p. 2200–2211 Vol. 84, No. 5
0022-538X/10/$12.00 doi:10.1128/JVI.00917-09

ICP27 Phosphorylation Site Mutants Are Defective in Herpes Simplex Virus 1 Replication and Gene Expression▽

Santos Rojas, Kara A. Corbin-Lickfett, Laurimar Escudero-Paunetto, and Rozanne M. Sandri-Goldin*

Department of Microbiology and Molecular Genetics, School of Medicine, University of California, Irvine, California 92697

Received 7 May 2009/Accepted 4 December 2009

Herpes simplex virus 1 (HSV-1) protein ICP27 is a multifunctional regulatory protein that is posttranslationally modified by phosphorylation during viral infection. ICP27 has been shown to be phosphorylated on three serine residues, specifically serine residues 16 and 18, which are within casein kinase 2 (CK2) sites, and serine residue 114, which is within a protein kinase A (PKA) site. Phosphorylation is an important regulatory mechanism that is reversible and controls many signaling pathways, protein-protein interactions, and protein subcellular localization. To determine the role of phosphorylation in modulating the activities of ICP27, we constructed phosphorylation site mutations at each of the three serine residues. Single, double, and triple viral mutants were created in which alanine or glutamic acid was substituted for serines 16, 18, and 114. ICP27 phosphorylation site mutants were defective in viral replication and viral gene expression. Notably, ICP4-containing replication compartment formation was severely compromised, with the appearance of small ring-like structures that persisted even at late times after infection. Neither the colocalization of ICP27 with RNA polymerase II nor the formation of Hsc70 nuclear foci was observed during infection with the phosphorylation site mutants, both of which occur during wild-type HSV-1 infection. These data indicate that several key events in which ICP27 plays a role are curtailed during infection with ICP27 phosphorylation site mutants.

Herpes simplex virus 1 (HSV-1) ICP27 is a multifunctional regulatory protein that interacts with a number of proteins and that binds RNA (32). The different activities of ICP27 are regulated in a temporal manner during infection. At early times, ICP27 is localized to the nucleus, whereas beginning about 5 to 6 h after infection, ICP27 continuously shuttles between the nucleus and cytoplasm. ICP27 mediates its nuclear activities through a series of protein-protein interactions. At very early times during infection, ICP27 recruits the predominantly cytoplasmic splicing factor kinase SRPK1 into the nucleus (34). This results in the aberrant phosphorylation of a family of essential splicing factors termed SR proteins, which are specifically phosphorylated by SRPK1. The inappropriate phosphorylation of SR proteins prevents their participation in spliceosome assembly, which causes splicing complex formation to stall, and host cell pre-mRNA splicing is impaired (15, 34). This contributes to the shutoff of host protein synthesis (14). Also at early times after infection, ICP27 interacts with the C-terminal domain (CTD) of RNA polymerase II (RNAP II) and causes RNAP II relocalization to sites of HSV-1 transcription/replication. This recruitment of RNAP II is necessary for highly active and efficient viral transcription (5). Beginning about 5 h after infection, ICP27 disassociates from splicing speckles, taking the cellular mRNA export factor Aly/REF with it to viral transcription/replication compartments (3, 4). ICP27 then binds viral transcripts (31) and facilitates their export to the cytoplasm through the TAP/NXF1 cellular mRNA export receptor, with which it interacts directly, as well as through its interaction with Aly/REF (3, 4, 18, 19). Once in the cytoplasm, ICP27 facilitates the translation of some viral transcripts through an interaction with translation initiation factors (7–9)

An important question to be addressed is how the various activities, subcellular localization, and protein interactions of ICP27 are regulated throughout infection. Posttranslational modifications such as phosphorylation and methylation have been shown to play important roles in regulating the intracellular distribution of proteins and in modulating protein-protein interactions. ICP27 is posttranslationally modified by phosphorylation (44) and arginine methylation (27, 38, 39). We showed recently that the methylation of ICP27 on three arginine residues within an RGG box motif is critical for regulating the export of ICP27 to the cytoplasm and for ICP27's functional interactions with SRPK1 and Aly/REF, which interact with ICP27 through a region that includes the RGG box (38, 39). Under conditions of hypomethylation in infections with arginine-to-lysine substitution mutants or in wild-type-infected cells in the presence of a methylation inhibitor, ICP27 was more rapidly exported to the cytoplasm at earlier times after infection, preventing ICP27 from performing its full array of nuclear functions and thus decreasing viral replication (38). Also, the interaction of SRPK1 and Aly/REF with ICP27 was impaired if ICP27 was hypomethylated, and these proteins were not recruited to the nucleus and to viral replication compartments, respectively (39). Thus, arginine methylation is an important regulator of ICP27 export and interaction with SRPK1 and Aly/REF.

Protein phosphorylation is an important posttranslational modification that regulates many cellular processes. Phosphorylation is a rapid and reversible process in which the negatively charged phosphate group modulates how the protein interacts with other molecules, both proteins and nucleic acids (10, 12, 16, 17, 20, 29). ICP27 is posttranslationally modified by phos-

* Corresponding author. Mailing address: Department of Microbiology & Molecular Genetics, School of Medicine, Medical Sciences, B240, University of California, Irvine, CA 92697-4025. Phone: (949) 824-7570. Fax: (949) 824-9054. E-mail: rmsandri@uci.edu.

▽ Published ahead of print on 16 December 2009.

phorylation (43, 44) on serine residues (44). We previously determined ICP27 sites that are phosphorylated during HSV-1 infection by phosphopeptide mapping studies (44). Casein kinase 2 (CK2) sites at serine residues 16 and 18, which are in the N-terminal leucine-rich region required for the export of ICP27, and serine residue 114, within a protein kinase A (PKA) site in the nuclear localization signal of ICP27, are extensively phosphorylated during infection (44). To determine the role of phosphorylation in regulating the various functions of ICP27, substitution mutations were introduced into ICP27 such that serine was replaced with alanine to resemble the unphosphorylated state or with glutamic acid to mimic the negative charge of a phosphate group. Viral mutants were constructed.

We characterized the growth properties of the ICP27 phosphorylation mutants and found that virus yields were reduced by 2 logs or more, and DNA replication and gene expression also were significantly reduced. Characteristic ICP4-containing replication compartments were not formed in mutant-infected cells, but instead small ring-like structures were observed. ICP27 did not colocalize with RNAP II in mutant-infected cells and the ICP27-mediated recruitment of Hsc70 to form nuclear foci did not occur, which together indicate that viral transcription was significantly reduced during infection with ICP27 phosphorylation site mutants.

MATERIALS AND METHODS

Cells and viruses. Vero cells were grown in minimal essential medium (MEM) with 8% fetal bovine serum and 4% donor calf serum at 37°C. Vero 2-2 cells were grown in MEM with 750 μg/ml G418 (36). HeLa cells were grown in MEM with 10% newborn calf serum. HSV-1 KOS and 27-LacZ were described previously (22, 36). ICP27 mutants dLeu and d1-5 (22) were provided by Steve Rice (University of Minnesota). ICP27 null mutant virus 27-GFP was described previously (41), as was N-YFP-ICP27 virus (18).

Recombinant plasmids. Plasmids pS16A, pS18A, and pS114A were described previously (44). ICP27 point mutations were created in plasmid pSG130B/S (35), which contains the full-length ICP27 sequence, using the QuikChange site-directed mutagenesis kit from Stratagene. Serine-to-alanine or serine-to-glutamic acid substitutions were made at residues 16, 18, and 114 with the primers S16,18A (5′CGGCCTGGACCTCGCCGACGCCGATCTG3′), S114A (5′GCCCGGCGACCGGCTTGCTCCCCCGAG3′), S16E (5′CCTCGGCCTGGACCTCGAAGACAGCGATCTG3′), S18E (5′GGACCTCTCCGACGAAGATCTGGACGAG3′), S114E (5′GCCCGGCGACCGGAATGCTCCCCCGAG3′), and S16,18E (5′CGGCCTGGACCTCGAAGACGAAGATCTG); S16,18,114E used primers for S16,18E and S114E. The altered nucleotides are underlined. Mutations were verified by DNA sequencing.

Construction of phosphorylation site mutants and rescued viruses. Phosphorylation site viral recombinants were constructed through homologous recombination as described previously (36). ICP27 phosphorylation site mutant plasmid DNA was digested with BamHI and SstI and cotransfected with 27-GFP viral DNA in 2-2 cells. Clear plaques were picked and purified for several rounds until green fluorescent plaques were absent. Viral mutant DNA was amplified by PCR, and the ICP27 gene was sequenced in each viral recombinant to verify the mutation. For rescued viruses, N-YFP-ICP27 plasmid DNA (18) was cotransfected with viral DNA isolated from phosphorylation site mutants into 2-2 cells. Yellow plaques were plaque purified five times and viral DNA was amplified by PCR, and the ICP27 gene was sequenced for each rescued virus.

Viral growth curves. Vero cells were infected with HSV-1 KOS, 27-GFP, N-YFP-ICP27, S16A, S18A, S114A, S16,18A, S16,18,114A, S16E, S18E, S114E, S16,18E, S16,18,114E, and rescued viruses S16AR, S114AR, and S16,18,114ER at a multiplicity of infection (MOI) of 1. At 0, 4, 8, 16, and 24 h after infection, infected cells were frozen at −80°C. Plaque assays were performed to determine the virus yield at each time point. Each experiment was performed two or three times. Growth curves for S16A, S114A, S16,18,114A, S16,18,114E, N-YFP-ICP27, and KOS also were performed in Vero cells and 2-2 cells as shown in Fig. 3. Cells were infected with each virus at an MOI of 1.0, and samples were frozen at 4, 8, 16, and 24 h after infection. Growth curves performed on Vero cells were assayed on Vero cells, and growth curves performed on 2-2 cells were assayed on 2-2 cells. Each experiment was performed twice.

Quantitative real-time PCR. HeLa cells were infected with HSV-1 KOS, 27-LacZ, S16A, S16E, S114A, S114E, S16,18,114A, and S16,18,114E at an MOI of 5. At 1 and 12 h after infection, cells were harvested and DNA was isolated by phenol-chloroform extraction. DNA was amplified with primers to the glycoprotein C (gC) gene using iQ Sybr green Supermix (Bio-Rad Laboratories) as previously described (19). For RNA isolation, infected cells were harvested at 4 and 8 h after infection and RNA was isolated using a Bio-Rad Laboratories total RNA kit (19). cDNA was synthesized using an iScript cDNA synthesis kit (Bio-Rad Laboratories) and amplified using primers for gC (19) and ICP8 (F5′-GACGGCAACCACCATCAAG-3′ and R5′-GACAGTAACGCCAGAAGC-3′) as described previously (19).

Western blot analysis. HeLa cells were infected with HSV-1 KOS, 27-LacZ, S18A, S18E, S114A, S114E, S16,18,114A, and S16,18,114E at an MOI of 5 for 4, 8, and 12 h. Cells were washed in phosphate-buffered saline (PBS) and scraped into 2× ESS as described previously (38, 39). Samples were fractionated by SDS-PAGE and transferred to nitrocellulose as described previously (33). Western blots were probed with the following primary antibodies: anti-ICP27 at a dilution of 1:5,000 (P1119; Virusys), anti-ICP4 at 1:5,000 (P1101; Virusys), and anti-β-actin at 1:10,000 (Sigma-Aldrich). The secondary antibody was horseradish peroxidase-conjugated sheep anti-mouse antibody. Enhanced chemiluminescence was performed (4).

***In vivo* phosphorylation and immunoprecipitation procedures.** HeLa cells were infected with HSV-1 KOS, 27-LacZ, S16,18,114A, S16,18,114E, dLeu, and d1-5 at an MOI of 5. Cells were radiolabeled with 50 μCi/ml [^{32}P]orthophosphate (Perkin Elmer) in phosphate-free MEM (44) beginning 45 min after infection for a period of 8 h. Cells were harvested and lysed in high-salt lysis buffer as described previously (31). Immunoprecipitation was performed as described previously (5, 44) using anti-ICP27 antibodies (P1113 and P1119; Virusys). Samples were fractionated on SDS-polyacrylamide gels and were transferred to nitrocellulose. Blots first were exposed to film. After the decay of the radiolabel, blots were probed with ICP27 antibody as previously described (44).

ICP27 protein stability assay. HeLa cells were infected at an MOI of 5 with HSV-1 KOS, d1-5, dLeu, S16,18,114A, or S16,18,114E. Whole-cell extracts were collected at 5, 6, 7, and 8 h postinfection either in the absence or the presence of 100 μg/ml cycloheximide added at 5 h. Samples were fractionated on SDS–10% polyacrylamide gels and transferred to nitrocellulose. Western blot analysis was performed using monoclonal antibodies to ICP27 (P1113 and P1119; Virusys) at a dilution of 1:5,000 and a monoclonal antibody to β-actin (Sigma) at a dilution of 1:10,000.

Immunofluorescence microscopy. HeLa cells were seeded on coverslips in 24-well dishes and were infected with KOS, 27-LacZ, S16A, S18A, S114A, S16,18A, S16,18,114A, S16E, S18E, S114E, S16,18E, and S16,18,114E at an MOI of 5. Cells were fixed with 3.7% formaldehyde at different times after infection as indicated in the legends to Fig. 5 to 8. Immunofluorescent staining was performed as described previously (5, 23) with the following primary antibodies: ICP27 (P1119; Virusys), ICP4 (P1101; Virusys), ARNA3 (Research Diagnostics), H5 (GeneTex Inc.), and Hsc70 (StressGen Biotechnologies). The secondary antibody was fluorescein isothiocyanate (FITC)-conjugated AffiniPure goat anti-mouse immunoglobulin M (IgM) (Jackson ImmunoResearch) or Texas Red dye-conjugated AffiniPure goat anti-mouse IgG. Cells were viewed with a Zeiss Axiovert S100 microscope or a Zeiss LSM 510 confocal microscope as indicated in the legends to Fig. 5 to 8. Images were analyzed with the following programs: Adobe Photoshop, LSM 510 image browser, and AxioVision 4.7.

RESULTS

ICP27 phosphorylation site mutants are defective in viral growth. To examine what role phosphorylation may have in regulating the activities of ICP27, we mutated three serine residues that previously were found to be extensively phosphorylated during viral infection by phosphopeptide analysis (44). Serine 16 and serine 18, within a consensus CK2 site in the leucine-rich region in the N terminus, and serine 114, within a PKA site in the nuclear localization signal, were mutated to alanine to mimic the unphosphorylated state and to glutamic acid to mimic the negative charge of a phosphate group (Fig. 1). Viral recombinants were constructed bearing single, dou-

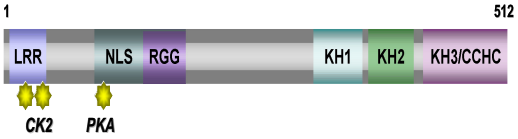

Mutant virus	Affected domain(s)	Amino acid alteration(s)
S16A	LRR	Residue 16, S to A
S18A	LRR	Residue 18, S to A
S114A	NLS	Residue 114, S to A
S16,18A	LRR	Residues 16 and 18, S to A
S16,18,114A	LRR, NLS	Residues 16, 18 and 114, S to A
S16E	LRR	Residue 16, S to E
S18E	LRR	Residue 18, S to E
S114E	NLS	Residue 114, S to E
S16,18E	LRR	Residues 16 and 18, S to E
S16,18,114E	LRR, NLS	Residues 16, 18 and 114, S to E

FIG. 1. Positions of the phosphorylation site mutations. Shown is a schematic representation of the ICP27 coding sequence illustrating the leucine-rich region (LRR) at the N terminus with CK2 sites denoted; the nuclear localization signal (NLS) with the PKA site denoted; the RGG box RNA binding domain; three predicted KH domains; and a zinc-finger-like region (CCHC). The mutant viruses are listed along with the affected domain and the amino acid substitution.

ble, and triple mutations (Fig. 1). One-step growth curves demonstrated that all of the mutants were impaired in viral replication, and virus yields were reduced 2 to 2.5 logs compared to those of wild-type HSV-1 KOS (Fig. 2A and B). Surprisingly, there were no significant differences in the defects in virus growth between the single and triple mutants or between alanine substitution mutants and glutamic acid substitution mutants. To ascertain that the substitution mutations were the cause of the phenotypes observed, the mutant viruses were rescued using plasmid DNA from N-YFP-ICP27, which has a yellow fluorescent protein (YFP) tag at the N terminus of ICP27 (18) for the recombination to allow the easier screening of rescued virus. One-step growth curves were performed (Fig. 3A to C). Rescued viruses S16AR, S114AR, and S16,18,114ER shown in Fig. 3A behaved similarly to N-YFP-ICP27 virus and to wild-type KOS. To further demonstrate that the substitution mutations caused the observed phenotypes, one-step growth curves were performed with mutants S16A, S114A, S16,18,114A, and S16,18,114E and compared to growth curves for N-YFP-ICP27 and KOS in Vero cells and in the complementing cell line 2-2. Growth curves performed with Vero cells were assayed on Vero cells, and growth curves performed with 2-2 cells were assayed on 2-2 cells (Fig. 3B and C). Yields of the phosphorylation site mutants on Vero cells were at least 2 logs lower than those of KOS and N-YFP-ICP27, which had equivalent yields (Fig. 3B), whereas the phosphorylation site mutants achieved yields equivalent to those of KOS and N-YFP-ICP27 on 2-2 cells (Fig. 3C). These results indicate that the substitution mutations,

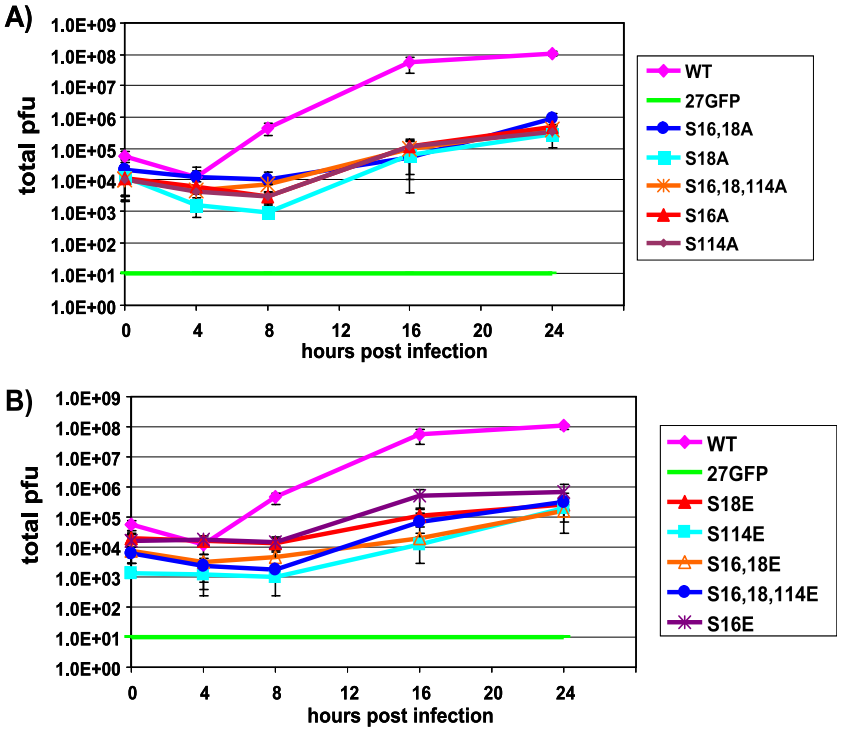

FIG. 2. Virus replication is reduced in ICP27 phosphorylation site mutant infection. (A) Vero cells were infected at an MOI of 1 with wild-type KOS, the null mutant 27-GFP, and the indicated alanine substitution mutants. Samples were harvested at 0, 4, 8, 16, and 24 h after infection. Virus titers were determined by plaque assays. (B) Vero cells were infected as described for panel A with wild-type KOS, 27-GFP, and the glutamic acid substitution mutants as indicated. Samples were harvested and assayed at 0, 4, 8, 16, and 24 h after infection as described for panel A. The experiments were performed three times, and error bars showing the standard deviations are shown.

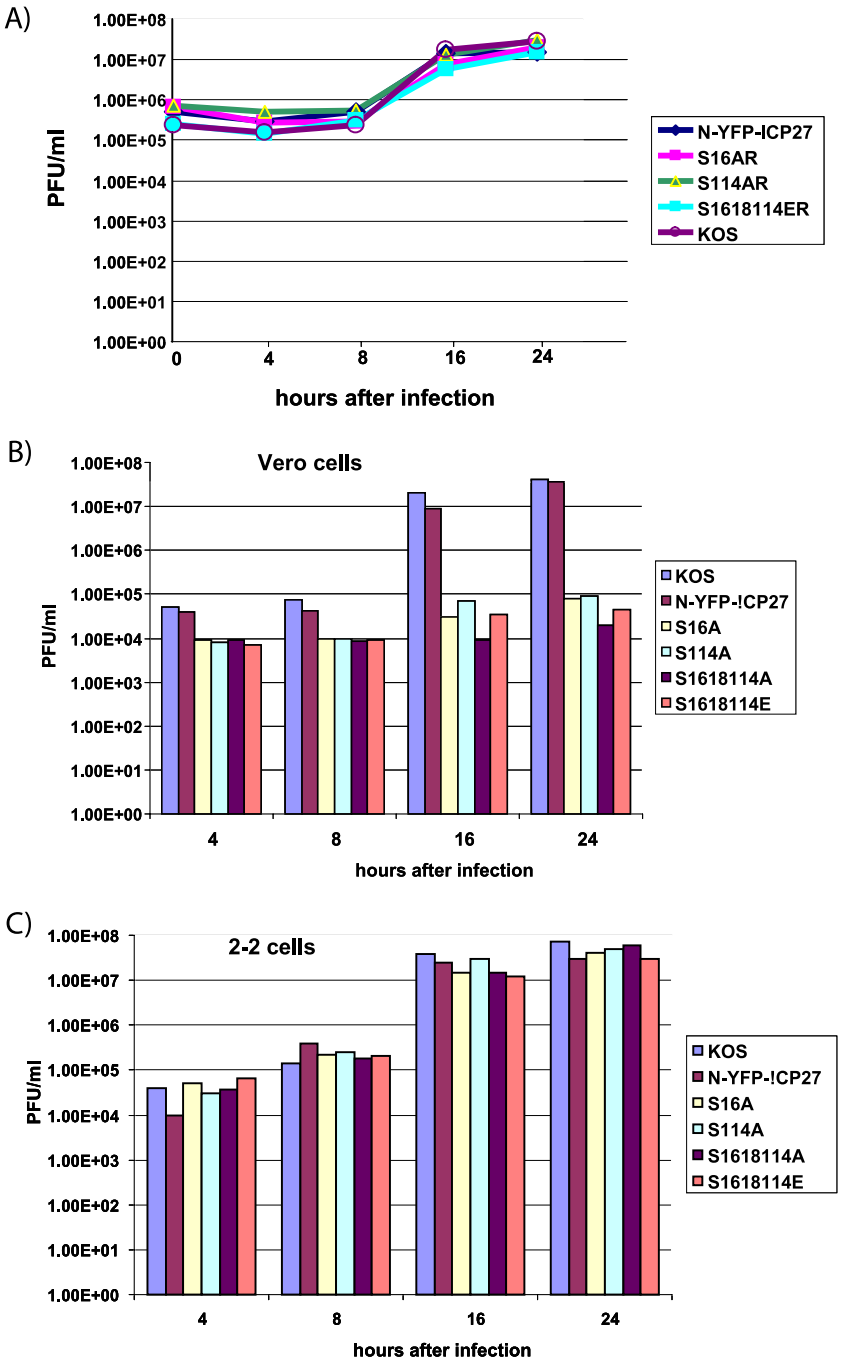

FIG. 3. Rescued phosphorylation site mutant viruses grow as well as wild-type KOS. (A) Vero cells were infected with KOS, N-YFP-ICP27, and the rescued viruses S16AR, S114AR, and S16,18,114ER at an MOI of 1. Samples were harvested at 0, 4, 8, 16, and 24 h after infection. Virus titers were determined by plaque assays on Vero cells. The experiment was repeated twice, and averages are shown. (B) Vero cells were infected with KOS, N-YFP-ICP27, and mutants S16A, S114A, S16,18,114A, and S16,18,114E at an MOI of 1, and samples were harvested at 4, 8, 16, and 24 h after infection. Virus titers were determined by assay on Vero cells. The experiments were performed twice, and the averages are shown. (C) Vero 2-2 cells were infected with KOS, N-YFP-ICP27, S16A, S114A, S16,18,114A, and S16,18,114E at an MOI of 1, and samples were harvested at 4, 8, 16, and 24 h after infection. Virus yields were determined by plaque assays on 2-2 cells. The experiments were performed twice, and the averages are shown.

and not second-site mutations, were responsible for the observed defects in viral replication.

Phosphorylation of mutants S16,18.114A and S16,18,114E is significantly decreased during infection. We showed previously that the major phosphorylation sites of ICP27 appeared to cluster in the N-terminal half of the protein (44). To determine if phosphorylation site mutants could be phosphorylated during infection, *in vivo* phosphorylation was monitored by

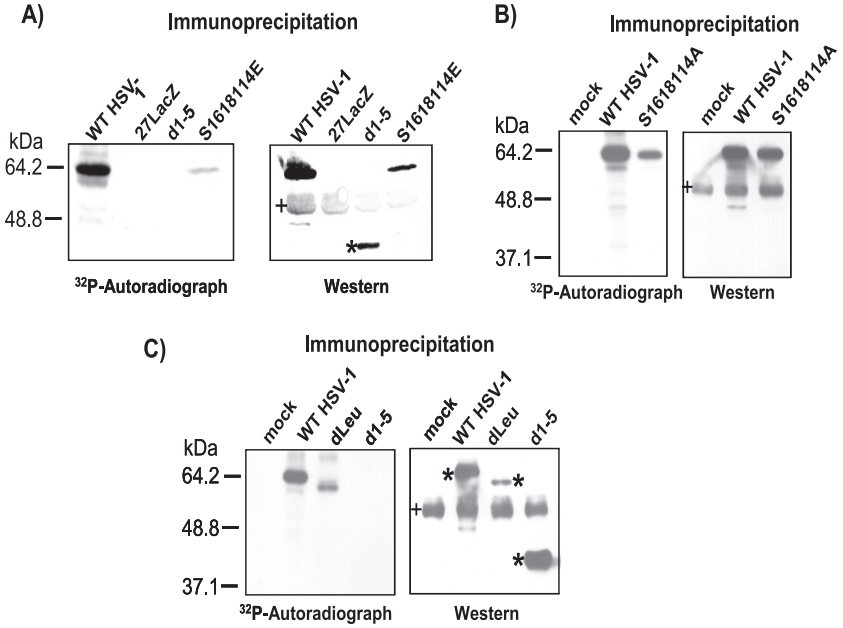

FIG. 4. *In vivo* phosphorylation of wild-type HSV-1 KOS and phosphorylation site mutants. (A) HeLa cells were infected with KOS, 27-LacZ, S16,18,114E, and d1-5 at an MOI of 5. Cells were labeled with [^{32}P]orthophosphate added 45 min after infection, and cells were harvested at 8 h after infection. Whole-cell lysates were immunoprecipitated with anti-ICP27 antibodies. Samples were fractionated by SDS-PAGE and transferred to nitrocellulose. The autoradiograph of the blot is shown in the left panel. After the decay of the radiolabel, the same blot was probed with antibody to ICP27 and is shown in the right panel. The asterisk marks the position of d1-5 protein. The bands denoted by the plus sign represent heavy-chain IgG from the immunoprecipitation. (B) HeLa cells were mock infected or were infected with KOS or S16,18,114A at an MOI of 5. *In vivo* labeling and Western blot analysis was performed as described for panel A. (C) HeLa cells were mock infected or were infected with HSV-1 KOS, dLeu, or d1-5 at an MOI of 5. Labeling and Western blot analysis were performed as described for panel A. The asterisks mark the position of wild-type and mutant ICP27. The bands denoted by the plus sign represent heavy-chain IgG from the immunoprecipitation.

adding [^{32}P]orthophosphate to cells infected with HSV-1 KOS, 27-LacZ, S16,18,114A, S16,18,114E, dLeu, or d1-5. The phosphorylation site triple mutants S16,18,114E and S16,18,114A were phosphorylated to a much lesser extent than wild-type ICP27 (Fig. 4A and B). The comparison of the amount of ICP27 that was immunoprecipitated to the amount of phosphorylation seen for S16,18,114E and S16,18,114A showed about a 10-fold decrease in phosphorylation for these mutants, whereas the amount of wild-type ICP27 phosphorylation was equivalent to the amount of immunoprecipitated protein (Fig. 4A and B). We also found that the phosphorylation of mutant dLeu protein appeared to be equivalent to the amount of immunoprecipitated protein, although dLeu has an in-frame deletion from amino acids 6 to 19 (22), removing the serines at 16 and 18 (Fig. 4C). These results indicate that there are other phosphorylation sites that are being used. We reported that ICP27 interacts with a splicing protein kinase, SRPK1, and that ICP27 can be phosphorylated *in vitro* by SRPK1 (34). Two predicted SRPK1 sites based upon the consensus recognition sequence for this kinase (28) map to ICP27 amino acids 28 to 33 and 70 to 76. ICP27 mutant d1-5 has an in-frame deletion of amino acids 12 to 153 (22), which removes the predicted SRPK1 phosphorylation sites, as well as the serine residues at positions 16, 18, and 114. In the *in vivo* phosphorylation experiment, phosphorylation was not detected for mutant d1-5 (Fig. 4A and C), confirming the phosphopeptide-mapping studies that indicated that ICP27 phosphorylation sites are clustered in the amino-terminal portion of the protein up to amino acid 163 (44). This experiment further demonstrates that serine residues 16, 18, and 114 are major phosphorylation sites for ICP27.

HSV-1 gene expression and DNA replication are reduced during infection with phosphorylation site mutants. To monitor the expression of two immediate-early proteins, ICP4 and ICP27 itself, a time course was performed, and Western blot analysis was used to assess protein levels in wild-type- and ICP27 mutant-infected cells (Fig. 5A). ICP4 protein levels were reduced about 3- to 4-fold compared to levels seen with KOS, and again no real differences were seen among the phosphorylation site mutants (Fig. 5A). ICP27 levels in the mutant infections were similar to those seen in KOS except for S16,18,114E and S114E, in which ICP27 levels were somewhat lower at 4 h compared to those of the other mutants but were comparable by 8 h (Fig. 5A). DNA replication in infections with S114A, S16A, S16,18,114A, S16E, S114E, and S16,18,114E, as measured by the real-time quantitative PCR of the gC locus, was greatly reduced compared to that of KOS at 12 h after infection (Fig. 5B). Further, both ICP8 and gC mRNA levels in the mutant infections were very low compared to those of KOS at 4 and 8 h after infection. Thus, although ICP4 levels were only moderately reduced compared to those of KOS, and ICP27 protein levels were only slightly reduced, there was a dramatic reduction in DNA replication and the expression of an early mRNA and a late mRNA in phosphorylation site mutant-infected cells.

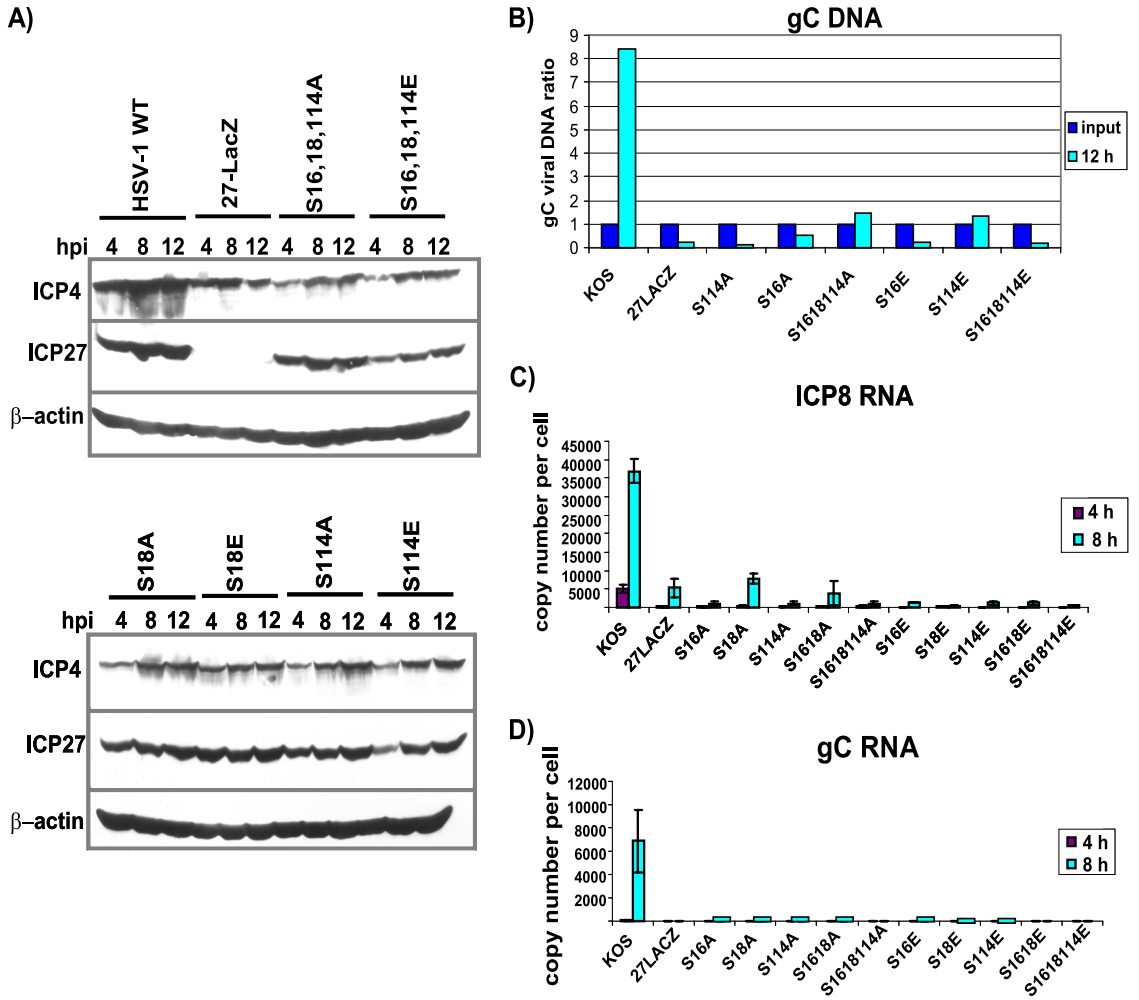

FIG. 5. DNA replication and gene expression are decreased in infections with ICP27 phosphorylation site mutants. (A) HeLa cells were infected with HSV-1 KOS, 27-LacZ, S16,18,114A, S16,18,114E, S18A, S18E, S114A, and S114E virus at an MOI of 5. Cells were harvested at 4, 8, and 12 h, and samples were fractionated by SDS-PAGE and transferred to nitrocellulose. Western blot analysis was performed by probing with anti-ICP4 and anti-ICP27 antibodies and with anti-β actin antibody as a loading control. (B) HeLa cells were infected with KOS, 27-LacZ, S16A, S18E, S114A, S114E, S16,18,114A, and S16,18,114E at an MOI of 5. At 1 and 12 h after infection, cells were harvested and viral DNA was isolated. Quantitative real-time PCR was used with probes to the gC locus to quantify viral DNA. DNA isolated at 1 h was set as the input, and the ratio of the 12-h samples to input samples was calculated. (C) HeLa cells were infected with the indicated viruses at an MOI of 5. RNA was isolated at 4 and 8 h after infection. ICP8 RNA was quantified by quantitative real-time RT-PCR using primers for ICP8. The experiment was performed three times, and error bars are shown. (D) Quantitative real-time RT-PCR was performed as described for panel C with primers for gC RNA. The experiment was performed three times, and error bars are shown.

ICP27 protein stability is not decreased in infections with the phosphorylation site mutants. We showed that the hypomethylation of ICP27, either by the mutation of arginine residues that are sites for arginine methylation or by the addition of the methylation inhibitor AdOx, reduced the stability of ICP27 (37). To determine if the serine-to-alanine or serine-to-glutamic acid mutations altered the stability of ICP27, protein stability was measured during infection with the phosphorylation site mutants. Cycloheximide was added to cells infected with HSV-1 KOS, S16,18,114A, S16,18,114E, dLeu, or d1-5 at 5 h after infection, and samples were analyzed by Western blot analysis 1, 2, and 3 h after the addition of the translation inhibitor (Fig. 6). No differences in the stability of ICP27 were seen with the phosphorylation site mutants compared to the stability of KOS (Fig. 6A and B), and ICP27 levels did not decrease during the cycloheximide block. We also determined the stability of the ICP27 mutant proteins dLeu and d1-5, because both have deletions that likely alter their structure and that could render these mutant proteins less stable. We did not observe a decrease in protein levels during the cycloheximide block with these mutants (Fig. 6C and D). Therefore, unlike the arginine methylation mutants, which were less stable than wild-type ICP27, the phosphorylation site mutants are not less stable.

ICP4-containing replication compartments form ring-like structures in phosphorylation site mutant-infected cells. To begin to determine where the blocks to HSV-1 replication occur during infection with ICP27 phosphorylation site mutants, replication compartment formation was monitored throughout infection by immunofluorescent staining for ICP4

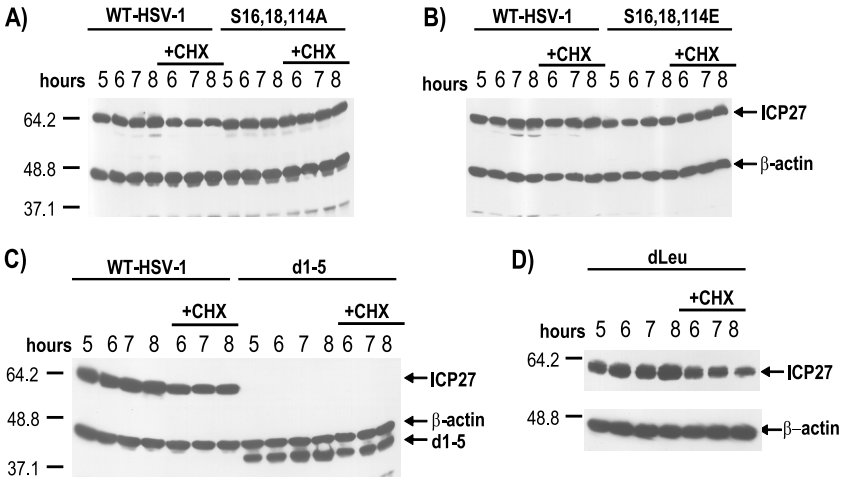

FIG. 6. ICP27 is not less stable in infections with the phosphorylation site mutants. HeLa cells were infected at an MOI of 5 with HSV-1 KOS, d1-5, dLeu, S16,18,114A, or S16,18,114E. Whole-cell extracts were collected at 5, 6, 7, and 8 h after infection either in the absence or the presence of 100 μg/ml cycloheximide added at 5 h after infection. Samples were fractionated on SDS–10% polyacrylamide gels and transferred to nitrocellulose. Western blot analysis was performed using monoclonal antibodies to ICP27. The positions of molecular size markers (in kDa) are shown to the left of the gels in panels A, C, and D.

(Fig. 7). Replication compartments were seen in KOS-infected cells by 8 h after infection, whereas small prereplication sites were observed in 27-LacZ-infected cells even up to 16 h after infection (Fig. 7A). In the single mutants S16A, S18A, and S114A and the double mutant S16,18A, small ring-like structures were seen to form beginning at 8 h after infection, which persisted through the 16 h time point above a background of diffuse nuclear staining (Fig. 7A). Similar results were seen with the mutants with glutamic acid substitutions (data not shown). These ring-like structures can be seen more clearly in the zoomed images for mutants S16,18,114A (Fig. 7B) and S16,18,114E (Fig. 7C). These ring-like structures clearly differ from prereplication sites reported by others (2, 26, 42) and from what we have observed with 27-LacZ (Fig. 7A) and with ICP27 mutants that are unable to interact with RNAP II (5). Importantly, true ICP4-containing replication compartments, as seen in KOS-infected cells, were not formed even at 16 h after infection with the phosphorylation site mutants.

ICP27 phosphorylation site mutants do not colocalize with RNA polymerase II. ICP27 interacts with RNAP II (5, 45) through the C-terminal domain (CTD), and ICP27 colocalizes with RNAP II (5). Therefore, we analyzed the localization of ICP27 and RNAP II in wild-type KOS and ICP27 mutant-infected cells by immunofluorescent staining. To stain RNAP II, antibody ARNA3 (5), which recognizes an N-terminal epitope of RNAP II, was used so that all forms of RNAP II, both phosphorylated and unphosphorylated, could be visualized. ICP27 and RNAP II were seen to colocalize in KOS-infected cells at 4 h after infection, and there still were areas of colocalization at 8 h when RNAP II was redistributed to replication compartments and ICP27 was shuttling between the nucleus and cytoplasm (Fig. 8). In contrast, while we observed some instances of ICP27 staining and RNAP II staining adjacent to each other, colocalization between ICP27 and RNAP II was not observed in cells infected with the phosphorylation site mutant S16E or S16,18,114E at 4 or 8 h after infection (Fig. 8). This can be seen more clearly in the zoomed images (Fig. 8). The same results were found for the alanine substitution mutants (data not shown). Therefore, ICP27 phosphorylation site mutant proteins appear to be unable to interact with RNAP II.

RNA polymerase II does not undergo degradation during infection with ICP27 phosphorylation site mutants, and Hsc70 nuclear foci do not form. During HSV-1 infection, RNAP II becomes redistributed from the diffuse nuclear fluorescence seen in mock-infected cells to viral replication compartments (5, 30). Although this result was found with KOS-infected cells (Fig. 9A), RNAP II remained diffusely distributed throughout the nuclei of S16E- and S16,18,114E-infected cells, with two or three small ring-like structures that colocalized with ICP4 rings (Fig. 9A). This result was found with the other phosphorylation site mutants as well (data not shown). Thus, during infection with phosphorylation site mutants, it appears that there is some redistribution of RNAP II to ICP4 ring-like structures, which may represent aberrant or poorly formed replication compartments, but most of the observed RNAP II appeared to be diffusely distributed throughout the nucleus.

We previously reported that during very active viral transcription in wild-type HSV-1-infected cells, RNAP II undergoes proteasomal degradation (5). It is the serine 2-phosphorylated form of the RNAP II CTD that is found in the elongating transcription complex that is degraded (5, 11), and this may result from the stalling of elongating complexes due to collisions or pile-ups during robust transcription in highly transcribed areas of the genome, as has been reported for *Saccharomyces cerevisiae* and mammalian cells (13, 21, 37). We and Fraser and Rice (11) have reported that in immunofluorescence studies of KOS-infected cells using monoclonal antibody H5, which is specific for the phosphoserine 2 CTD (6), there was a disappearance of the diffuse staining seen in mock-infected cells, and instead H5 staining colocalized with splicing speckles (5, 11). The colocalization with splicing speckles occurred because antibody H5 has been shown to cross-react with a phosphoepitope in SR splicing proteins under conditions in which the serine 2-phosphorylated form of RNAP II CTD is

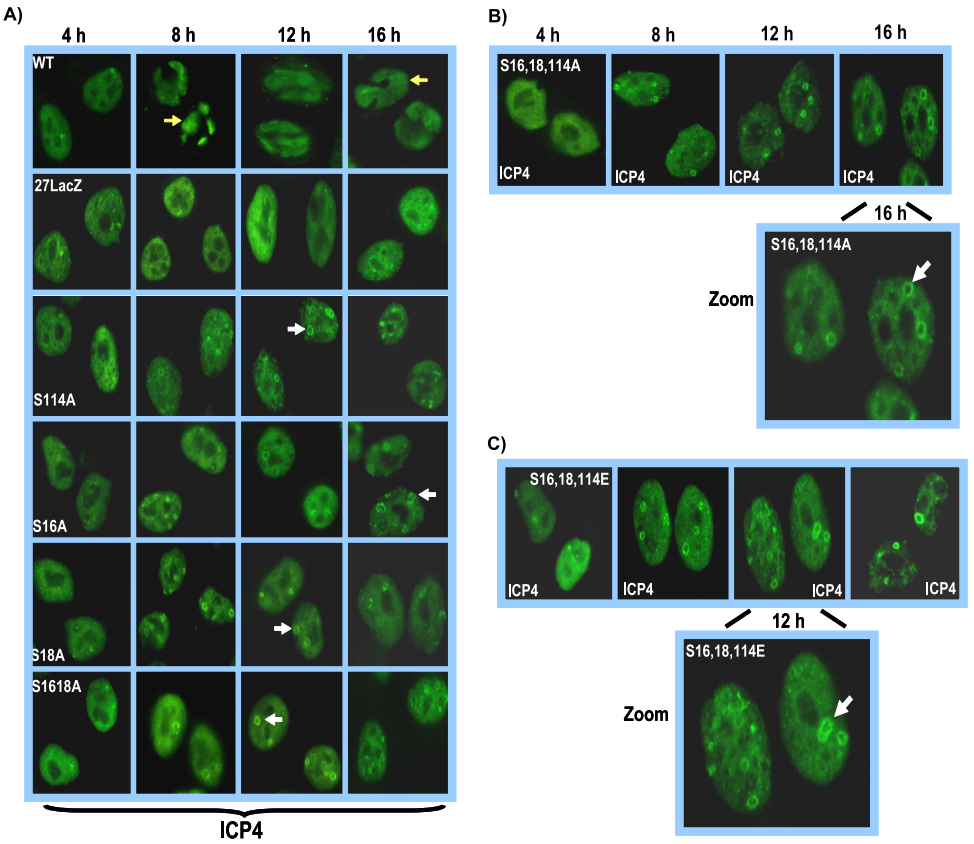

FIG. 7. ICP4-containing replication compartment formation is reduced in ICP27 phosphorylation site mutant infections. (A) HeLa cells were infected with wild-type KOS, 27-LacZ, S16A, S18A, S114A, and S16,18A at an MOI of 5. Cells were fixed and stained with anti-ICP4 antibody at 4, 8, 12, and 16 h after infection. Yellow arrows point to ICP4-containing globular transcription/replication compartments in wild-type KOS-infected cells at 8 and 16 h after infection. White arrows point to ICP4 ring-like structures seen in the phosphorylation mutant infections. (B) HeLa cells were infected as described for panel A with S16,18,114A, and cells were fixed and stained at the times indicated in the figure. The image at 16 h after infection has been zoomed to view the ICP4 ring-like structures denoted by the white arrow. (C) Cells were infected with S16,18,114E as described for panel A. The image at 12 h has been zoomed to better demonstrate the ICP4 ring-like structures. The white arrow points to a ring-like structure.

decreased and is less abundant than SR proteins, which are very abundant splicing proteins (6). Therefore, as we showed previously (5, 23), staining with antibody H5 can be used as an assay to assess the degradation of the serine 2 form of the RNAP II CTD. Under conditions in which the phosphoserine 2 form of the CTD is being degraded, antibody H5 will cross-react with SR proteins and stain splicing speckles. Accordingly, mock-infected cells and cells infected with wild-type KOS and mutant S16,18,114E were stained with antibody H5 at 8 h after infection, a time when the significant degradation of the serine 2-phosphorylated form has occurred in wild-type KOS-infected cells (5, 23). As seen in Fig. 9B, a speckled staining pattern was found in KOS-infected cells, indicating that the phosphoserine 2 form of the CTD was being degraded, and antibody H5 cross-reacted with SR proteins in splicing speckles (Fig. 9B). In contrast, the H5 staining pattern was diffuse throughout the nucleus in S16,18,114E-infected cells, similarly to what is seen in mock-infected cells (Fig. 9B). The lack of the degradation of the serine 2-phosphorylated RNAP II CTD indicates that viral transcription during S16,18,114E infection was greatly reduced, so that collisions or pile-ups causing stalled RNAP II complexes did not occur. We have demonstrated that this is the case for ICP27 mutants that cannot interact with RNAP II and that have very low levels of viral transcription (5). The data shown in Fig. 4 for ICP8 and gC mRNA also indicate that viral transcription is reduced in phosphorylation site mutant infections.

During HSV-1 infection, the chaperone protein Hsc70 is sequestered in nuclear foci that lie at the periphery of viral replication compartments (1, 23). These foci, which also have been termed VICE domains (for virus-induced-chaperone-enriched), also contain other heat shock proteins as well as components of the proteasomal and ubiquitination machineries (1). These foci may serve as reservoirs so that these factors can be easily accessible to mediate the ubiquitination and proteasomal degradation of misfolded viral proteins (1, 24) and stalled RNAP II complexes (23). We reported that ICP27 is required for the recruitment of Hsc70 into nuclear foci (23), and further that Hsc70 focus formation did not occur if RNAP II degradation was blocked by proteasomal inhibitors or by the expression of a dominant-negative form of Hsc70 (23). To determine if Hsc70 was recruited into nuclear foci or VICE domains during infection with ICP27 phosphorylation site mutants, immunofluorescent staining was performed. In KOS-

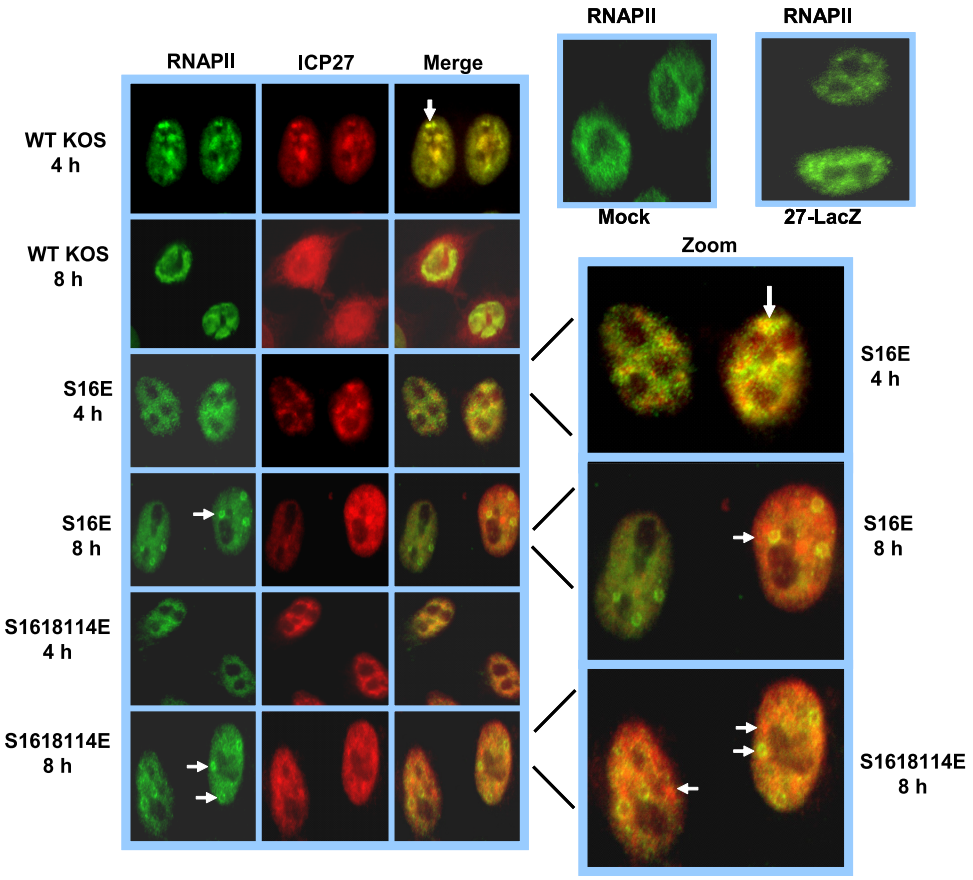

FIG. 8. ICP27 does not colocalize with RNAP II in cells infected with phosphorylation site mutants. HeLa cells were infected with wild-type KOS, S16E, and S16,18,114E at an MOI of 5 for 4 and 8 h as indicated. Cells were fixed, and immunofluorescent staining was performed with anti-RNAP II antibody ARNA3 and anti-ICP27 antibody. Images were visualized with a Zeiss Axiovert S100 microscope at a magnification of ×100. Arrows point to the areas of colocalization in wild-type KOS at 4 h after infection and to areas where colocalization was not seen in the zoomed images for S16E at 4 h and S16,18,114E at 8 h.

infected cells, Hsc70 foci were seen at the periphery of ICP4-containing replication compartments at 8 h after infection (Fig. 10). In contrast, Hsc70 was seen to be diffusely distributed throughout the nucleus and cytoplasm of mock-infected cells and in 27-LacZ-infected cells. Similarly, in cells infected with S16E, S18E, S114E, and S16,18,114E, Hsc70 was diffusely distributed throughout the nucleus and cytoplasm and nuclear foci were not apparent (Fig. 10, right). This result is another indication that viral transcription is reduced in infection with phosphorylation site mutants, because one role for these nuclear foci or VICE domains is to direct stalled RNAP II complexes to proteasomal degradation (23).

DISCUSSION

Phosphorylation is an important posttranslational modification that can regulate the activities and interactions of proteins. HSV-1 ICP27 is a multifunctional protein that has many different roles during viral infection, all of which involve ICP27 binding to proteins or RNA (32). To probe how ICP27 switches from one interaction to another, we mutated three major phosphorylation sites and analyzed the consequences on viral replication. Virus growth, DNA replication, and the transcription of an early and late mRNA were greatly reduced in all of the phosphorylation site mutant infections. We had expected that there would be differences among the mutants, with a less severe phenotype found with the single mutants compared to that of the triple mutants. This was in fact what we found when we investigated the posttranslational arginine methylation of the ICP27 RGG box (38). Single mutants were somewhat more replication competent than double and triple mutants. It also was predicted that there would be a phenotypic difference between the alanine substitution mutants and the glutamic acid substitution mutants. The alanine mutants would be more similar to unphosphorylated serine, whereas the negatively charged glutamic acid would be more similar to phosphorylated serine. Thus, unphosphorylated ICP27 would be expected to undergo one set of interactions, whereas phosphorylated ICP27 might undergo another set. For example, the yeast shuttling protein Npl3p, which is involved in mRNA export (12), is phosphorylated at a single serine residue at the C terminus, which is important for its nuclear import. In the nucleus, Npl3p is dephosphorylated, which is essential for its recruitment of the yeast nuclear export receptor Mex67p to the Npl3p/mRNP complex for export to the cytoplasm (12, 25).

In the processes that were monitored here, the ICP27 phos-

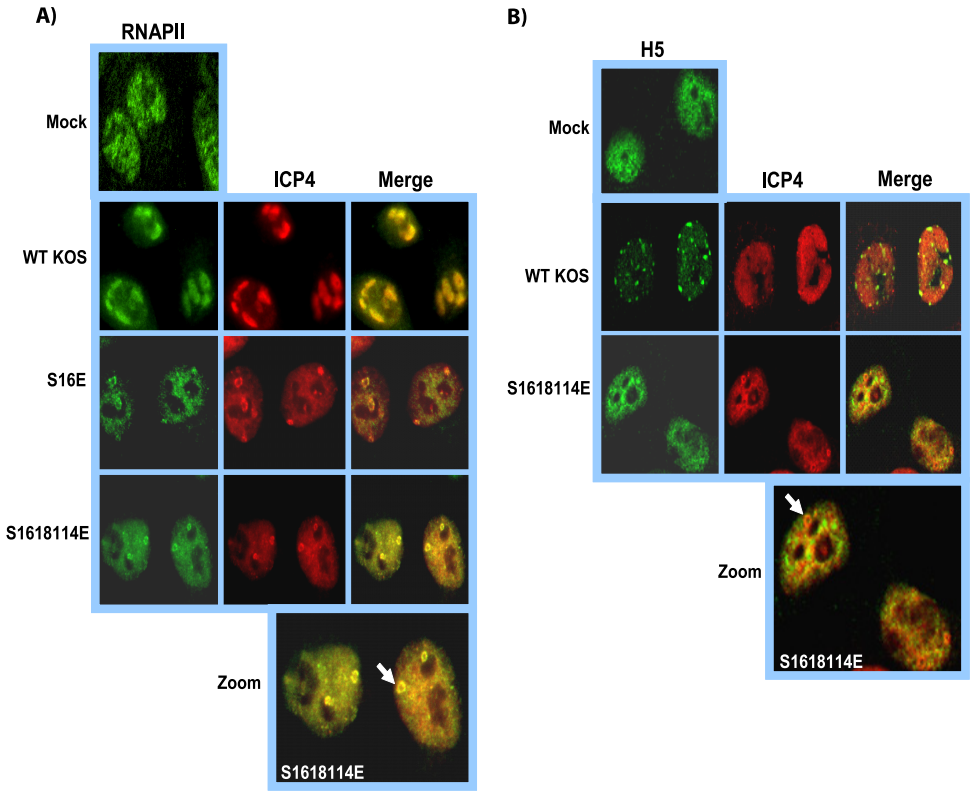

FIG. 9. RNAP II was partly localized to ring-like structures and did not undergo degradation in phosphorylation site mutant infections. (A) HeLa cells were mock infected or were infected with KOS, S16E, and S16,18,114E at an MOI of 5 for 8 h, at which time cells were fixed and immunofluorescent staining was performed with antibody ARNA3 and anti-ICP4 antibody. Images were visualized with a Zeiss Axiovert S100 microscope at a magnification of ×100. The arrow points to a ring-like structure in the zoomed image. (B) HeLa cells were mock infected or were infected with KOS or S16,18,114 at an MOI of 5 for 8 h. Immunofluorescent staining was performed with antibody H5 and anti-ICP4 antibody. Images were visualized with a Zeiss LSM 510 confocal microscope at a magnification of ×63. The arrow points to an ICP4 ring-like structure in the zoomed image.

phorylation mutants did not display differences. Replication compartment formation was aberrant, in that the large globular structures that contain ICP4, which are found in wild-type HSV-1-infected cells (2, 26, 30, 40, 42), were not seen. Instead, small ring-like structures were seen in infections with the phosphorylation site mutants. Even as late as 16 h after infection, these were the only discernible structures above a background of diffuse ICP4 staining. ICP27 phosphorylation mutant proteins also did not colocalize with RNAP II, and RNAP II was not redistributed to viral replication compartments, as occurs in KOS-infected cells (5, 30), but instead was found in a diffuse nuclear pattern with a few structures that colocalized with ICP4 ring-like structures. We showed previously using microarray analysis that viral transcript levels are reduced to about 10% of wild-type KOS levels during infection with ICP27 mutants that cannot recruit RNAP II to viral transcription/replication sites (5). In phosphorylation site mutant infections, low levels of ICP8 and gC transcripts were found in accord with the aberrant replication compartment formation and the lack of the redistribution of RNAP II that was observed. Another indication that viral transcription was reduced in ICP27 phosphorylation site mutants was the finding that the serine 2 form of the RNAP II CTD was not degraded, as occurs during robust transcription in wild-type HSV-1 infection (5). This also was manifested in the absence of Hsc70 nuclear foci in infections with the phosphorylation site mutants. Hsc70 was diffusely distributed throughout the nucleus and cytoplasm of ICP27 mutant-infected cells, as it is in mock-infected cells.

The results reported here demonstrate that viral infection is curtailed at an early stage during infection with ICP27 phosphorylation site mutants. The levels of ICP4 were only modestly decreased, but ICP4 remained diffusely localized throughout the nucleus, with only a few ring-like structures that formed and that may represent aberrant or poorly developed replication compartments. Further, the ICP27 recruitment of RNAP II to viral transcription-replication sites is required for efficient viral transcription (5). Again, this did not occur in infections with ICP27 phosphorylation site mutants. The interaction of ICP27 with RNAP II and Hsc70 require that the N terminus be intact (5, 23), and serine 16 and serine 18 are within the region that interacts with these proteins, although serine 114 is not. The alanine and glutamic acid substitution mutants behaved similarly, leading us to postulate that conformational changes that occur at these sites by the addition and subsequent removal of a phosphate group may regulate ICP27's protein-protein interactions. Both the alanine and glutamic acid substitution mutants may be held in a conformation that affects the entire N-terminal region and that does not allow flexibility in ICP27's interactions. Results from nuclear

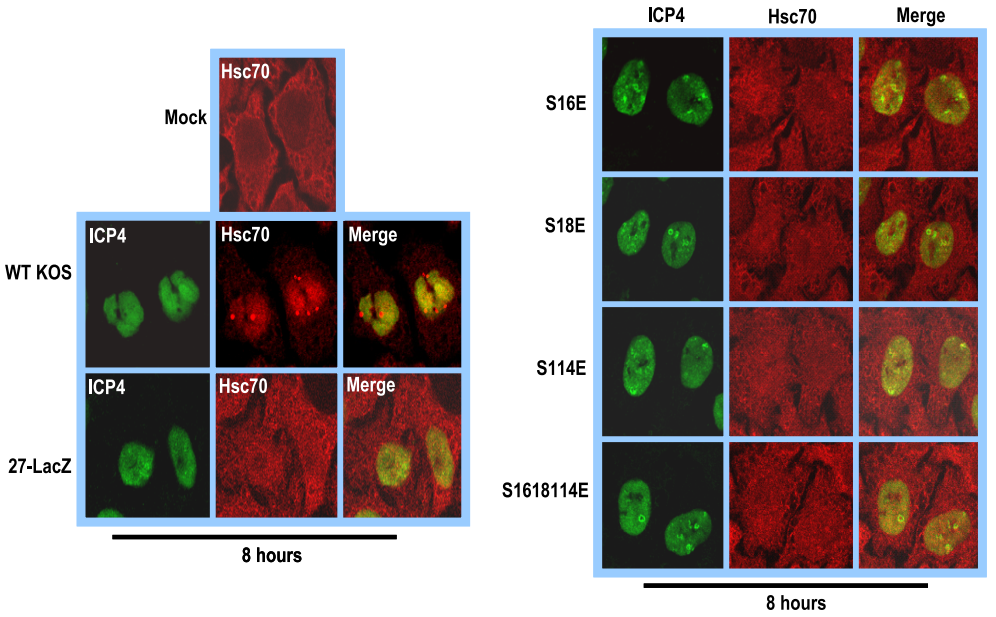

FIG. 10. Hsc70 focus formation was not observed in infections with ICP27 phosphorylation site mutants. HeLa cells were mock infected or were infected with KOS, S16E, S18E, S114E, and S16,18,114E at an MOI of 5. At 8 h after infection, cells were fixed and stained with anti-Hsc70 and anti-ICP4 antibodies. Images were visualized with the Zeiss LSM 510 confocal microscope at a magnification of ×63.

magnetic resonance analysis of an ICP27 peptide from amino acid 1 through 152 that will be reported elsewhere suggest that this is the case (K. Corbin-Lickfett, S. Rojas, M. Cocco, and R. M. Sandri-Goldin, unpublished results).

ACKNOWLEDGMENTS

We thank Steve Rice for providing ICP27 mutants dLeu and d1-5.

This work was supported by the National Institute of Allergy and Infectious Diseases (NIAID) grants AI61397 and AI21215.

REFERENCES

1. **Burch, A. D., and S. K. Weller.** 2004. Nuclear sequestration of cellular chaperone and proteasomal machinery during herpes simplex virus type 1 infection. J. Virol. **78:**7175–7185.
2. **Burkham, J., D. M. Coen, and S. K. Weller.** 1998. ND10 protein PML is recruited to herpes simplex virus type 1 prereplicative sites and replication compartments in the presence of viral DNA polymerase. J. Virol. **72:**10100–10107.
3. **Chen, I. B., L. Li, L. Silva, and R. M. Sandri-Goldin.** 2005. ICP27 recruits Aly/REF but not TAP/NXF1 to herpes simplex virus type 1 transcription sites although TAP/NXF1 is required for ICP27 export. J. Virol. **79:**3949–3961.
4. **Chen, I. B., K. S. Sciabica, and R. M. Sandri-Goldin.** 2002. ICP27 interacts with the export factor Aly/REF to direct herpes simplex virus 1 intronless RNAs to the TAP export pathway. J. Virol. **76:**12877–12889.
5. **Dai-Ju, J. Q., L. Li, L. A. Johnson, and R. M. Sandri-Goldin.** 2006. ICP27 interacts with the C-terminal domain of RNA polymerase II and facilitates its recruitment to herpes simplex virus-1 transcription sites, where it undergoes proteasomal degradation during infection. J. Virol. **80:**3567–3581.
6. **Doyle, O., J. L. Corden, C. Murphy, and J. G. Gall.** 2002. The distribution of RNA polymerase II largest subunit (RPB1) in the *Xenopus* germinal vesicle. J. Struct. Biol. **140:**154–166.
7. **Ellison, K. S., R. A. Maranchuk, K. L. Mottet, and J. R. Smiley.** 2005. Control of VP16 translation by the herpes simplex virus type 1 immediate-early protein ICP27. J. Virol. **79:**4120–4131.
8. **Fontaine-Rodriguez, E. C., and D. M. Knipe.** 2008. Herpes simplex virus ICP27 increases translation of a subset of viral late mRNAs. J. Virol. **82:**3538–3545.
9. **Fontaine-Rodriguez, E. C., T. J. Taylor, M. Olesky, and D. M. Knipe.** 2004. Proteomics of herpes simplex virus infected cell protein 27: association with translation initiation factors. Virology **330:**487–492.
10. **Fouts, D. E., H. I. True, K. A. Cengel, and D. W. Celander.** 1997. Site-specific phosphorylation of the human immunodeficiency virus type −1 Rev protein accelerates formation of an efficient RNA-binding conformation. Biochemistry **36:**13256–13262.
11. **Fraser, K. A., and S. A. Rice.** 2005. Herpes simplex virus type 1 infection leads to loss of serine-2 phosphorylation on the carboxyl-terminal domain of RNA polymerase II. J. Virol. **79:**11323–11334.
12. **Gilbert, W., C. W. Siebel, and C. Guthrie.** 2001. Phosphorylation by Sky1p promotes Np13p shuttling and mRNA dissociation. RNA **7:**302–313.
13. **Gillette, T. G., F. Gonzalez, A. Delahodde, S. A. Johnston, and T. Kodadek.** 2004. Physical and functional association of RNA polymerase II and the proteasome. Proc. Natl. Acad. Sci. USA **101:**5904–5909.
14. **Hardwicke, M. A., and R. M. Sandri-Goldin.** 1994. The herpes simplex virus regulatory protein ICP27 can cause a decrease in cellular mRNA levels during infection. J. Virol. **68:**4797–4810.
15. **Hardy, W. R., and R. M. Sandri-Goldin.** 1994. Herpes simplex virus inhibits host cell splicing, and regulatory protein ICP27 is required for this effect. J. Virol. **68:**7790–7799.
16. **Hsu, I., M. Hsu, C. Li, T. Chuang, R. Lin, and W.-Y. Tarn.** 2005. Phosphorylation of Y14 modulates its interaction with proteins involved in mRNA metabolism and influences its methylation. J. Biol. Chem. **280:**34507–34512.
17. **Jans, D. A.** 1995. The regulation of protein transport to the nucleus by phosphorylation. Biochem. J. **311:**705–716.
18. **Johnson, L. A., L. Li, and R. M. Sandri-Goldin.** 2009. The cellular RNA export receptor TAP/NXF1 is required for ICP27-mediated export of herpes simplex virus 1 RNA, whereas the TREX-complex adaptor protein Aly/REF appears to be dispensable. J. Virol. **83:**6335–6346.
19. **Johnson, L. A., and R. M. Sandri-Goldin.** 2009. Efficient nuclear export of herpes simplex virus 1 transcripts requires both RNA binding by ICP27 and ICP27 interaction with TAP/NXF1. J. Virol. **83:**1184–1192.
20. **Johnson, L. N., and R. J. Lewis.** 2001. Structural basis for control by phosphorylation. Chem. Rev. **101:**2209–2242.
21. **Kleiman, F. E., F. Wu-Baer, D. Fonseca, S. Kaneko, and R. Baer.** 2005. BRCA1/BARD1 inhibition of mRNA 3′ processing involves targeted degradation of RNA polymerase II. Genes Dev. **19:**1227–1237.
22. **Lengyel, J., C. Guy, V. Leong, S. Borge, and S. A. Rice.** 2002. Mapping of functional regions in the amino-terminal portion of the herpes simplex virus ICP27 regulatory protein: importance of the leucine-rich nuclear export signal and RGG box RNA-binding domain. J. Virol. **76:**11866–11879.
23. **Li, L., L. A. Johnson, J. Q. Dai-Ju, and R. M. Sandri-Goldin.** 2008. Hsc70 focus formation at the periphery of HSV-1 transcription sites requires ICP27. PLoS One **3:**e1491.
24. **Livingston, C. M., M. F. Ifrim, A. E. Cowan, and S. K. Weller.** 2009. Virus-induced chaperone-enriched (VICE) domains function as nuclear protein quality control centers during HSV-1 infection. PLoS Pathog. **5:**e1000619.
25. **Lukasiewicz, R., B. Nolen, J. A. Adams, and G. Ghosh.** 2007. The RGG domain of Npl3 recruits Sky1p through docking interactions. J. Mol. Biol. **367:**249–261.
26. **Lukonis, C. J., and S. K. Weller.** 1997. Formation of herpes simplex virus

type 1 replication compartments by transfection: requirements and localization to nuclear domain 10. J. Virol. **71:**2390–2399.
27. **Mears, W. E., and S. A. Rice.** 1996. The RGG box motif of the herpes simplex virus ICP27 protein mediates an RNA-binding activity and determines in vivo methylation. J. Virol. **70:**7445–7453.
28. **Nolen, B., C. Y. Yun, C. F. Wong, J. A. McCammon, X. D. Fu, and G. Ghosh.** 2001. The structure of Sky1p reveals a novel mechanism for constitutive activity. Nat. Struct. Biol. **8:**176–183.
29. **Patton, E., A. Steeler, and S. Ceman.** 2005. The role of phosphorylation in regulating FMRP function, p. 229–243. *In* Y. J. Sung and R. B. Denman (ed.), The molecular basis of fragile-X syndrome. Research Signpost, Kerala, India.
30. **Rice, S. A., M. C. Long, V. Lam, and C. A. Spencer.** 1994. RNA polymerase II is aberrantly phosphorylated and localized to viral replication compartments following herpes simplex virus infection. J. Virol. **68:**988–1001.
31. **Sandri-Goldin, R. M.** 1998. ICP27 mediates herpes simplex virus RNA export by shuttling through a leucine-rich nuclear export signal and binding viral intronless RNAs through an RGG motif. Genes Dev. **12:**868–879.
32. **Sandri-Goldin, R. M.** 2008. The many roles of the regulatory protein ICP27 during herpes simplex virus infection. Front. Biosci. **13:**5241–5256.
33. **Sandri-Goldin, R. M., and M. K. Hibbard.** 1996. The herpes simplex virus type 1 regulatory protein ICP27 coimmunoprecipitates with anti-Sm antiserum and, the C terminus appears to be required for this interaction. J. Virol. **70:**108–118.
34. **Sciabica, K. S., Q. J. Dai, and R. M. Sandri-Goldin.** 2003. ICP27 interacts with SRPK1 to mediate HSV-1 inhibition of pre-mRNA splicing by altering SR protein phosphorylation. EMBO J. **22:**1608–1619.
35. **Sekulovich, R. E., K. Leary, and R. M. Sandri-Goldin.** 1988. The herpes simplex virus type 1 alpha protein ICP27 can act as a trans-repressor or a trans-activator in combination with ICP4 and ICP0. J. Virol. **62:**4510–4522.
36. **Smith, I. L., M. A. Hardwicke, and R. M. Sandri-Goldin.** 1992. Evidence that the herpes simplex virus immediate early protein ICP27 acts posttranscriptionally during infection to regulate gene expression. Virology **186:**74–86.
37. **Somesh, B., J. Reid, W. Liu, T. M. M. Sogaard, H. Erdjument-Bromage, P. Tempst, and J. Q. Svejstrup.** 2005. Multiple mechanisms confining RNA polymerase II ubiquitylation to polymerases undergoing transcriptional arrest. Cell **121:**913–923.
38. **Souki, S. K., P. D. Gershon, and R. M. Sandri-Goldin.** 2009. Arginine methylation of the ICP27 RGG box regulates ICP27 export and is required for efficient herpes simplex virus 1 replication. J. Virol. **83:**5309–5320.
39. **Souki, S. K., and R. M. Sandri-Goldin.** 2009. Arginine methylation of the ICP27 RGG box regulates the functional interactions of ICP27 with SRPK1 and Aly/REF during herpes simplex virus 1 infection. J. Virol. **83:**8970–8975.
40. **Sourvinos, G., and R. D. Everett.** 2002. Visualization of parental HSV-1 genomes and replication compartments in association with ND10 in live infected cells. EMBO J. **21:**4989–4997.
41. **Sun, A., G. V. Devi-Rao, M. K. Rice, L. W. Gary, D. C. Bloom, R. M. Sandri-Goldin, P. Ghazal, and E. K. Wagner.** 2004. Immediate-early expression of the herpes simplex virus type 1 ICP27 transcript is not critical for efficient replication in vitro or in vivo. J. Virol. **78:**10470–10478.
42. **Taylor, T. J., E. E. McNamee, C. Day, and D. M. Knipe.** 2003. Herpes simplex virus replication compartments can form by coalescence of smaller compartments. Virology **309:**232–247.
43. **Wilcox, K. W., A. Kohn, E. Sklyanskaya, and B. Roizman.** 1980. Herpes simplex virus phosphoproteins. I. Phosphate cycles on and off some viral polypeptides and can alter their affinity for DNA. J. Virol. **33:**167–182.
44. **Zhi, Y., and R. M. Sandri-Goldin.** 1999. Analysis of the phosphorylation sites of the herpes simplex virus type 1 regulatory protein ICP27. J. Virol. **73:** 3246–3257.
45. **Zhou, C., and D. M. Knipe.** 2002. Association of herpes simplex virus 1 ICP8 and ICP27 with cellular RNA polymerase II holoenzyme. J. Virol. **76:**5893–5904.